Progress In Electromagnetics Research Letters, Vol. 99, 111–118, 2021

Low Profile Wide Beamwidth Antenna Fed by 1 : 5 Unequal Wilkinson Power Divider

Anfu Zhu[1], Sifan Wu[2], Junwei Shi[2], Peng Hu[2], and Jianxing Li[2, *]

Abstract—A novel wide beamwidth microstrip patch antenna fed by a 1 : 5 unequal Wilkinson power divider with a low profile of $0.027\lambda_0$ is presented. A circular patch and an independent feeding concentric metal ring can realize the broad half-power beamwidth (HPBW) in the far field. A 1 : 5 unequal Wilkinson power divider is designed as the antenna feed. The HPBWs of the antenna reach 258° and 267° in XZ-plane and YZ-plane, respectively, covering the whole upper half space at central frequency (2.54 GHz). The results of simulation and measurement show great consistency.

1. INTRODUCTION

With the development of communication system towards integration, higher requirements are put forward for miniaturization of antennas. Microstrip antennas have great advantages in cost, fabrication technology, and conformal ability [1–5]. The research of low profile antennas has a broad prospect in engineering applications.

Narrow HPBW limits the efficiency of radio frequency identification (RFID) systems [6]. There are some researches to broaden the half-power beamwidth. The HPBW of 140° is achieved through a parasitic ring. However, due to the double layer structure, the height of profile is $0.11\lambda_0$ [7]. Higher-mode resonance is utilized to broaden the E-plane HPBW of the patch antenna with a large size of $1.2\lambda_0 \times 1.2\lambda_0$ and obtains a 118% HPBW [8]. Furthermore, the backed cavity is used to broaden HPBW [9, 10], but it results in mass waviness in the radiation pattern and a high profile. In [11], for a microstrip antenna, the dielectric substrate extends out relative to the metal ground. As a result, a wider HPBW has been achieved. In [12], four unbalanced circular patches use coupled shorting strip and capacitive probe as feeding which achieve 170° HPBW. However, space utilization of the antenna is not good because of the design of the feed network. In [13], the work gives a scheme to broaden the HPBW but does not achieve the antenna feed network.

In this paper, a low profile wide beamwidth microstrip patch antenna is proposed. A coplanar concentric metal ring is used to broaden the beamwidth. Furthermore, a 1 : 5 unequal Wilkinson power divider is designed to feed the antenna. The half-power beamwidth can cover the entire upper half space. The result shows that the HPBWs of the antenna reach 258° and 267° respectively in the two vertical planes at central frequency (2.54 GHz). The antenna has been simulated using CST 2019 and demonstrated by experiments.

2. ANTENNA DESIGN

Figure 1(a) shows the configuration of the proposed antenna. A patch and a concentric annular ring are printed on a Taconic RF-60 substrate ($\varepsilon_r = 6.15$, $\tan\delta = 0.0028$, $h = 3.18$ mm) with a radius of 43 mm.

Received 13 April 2021, Accepted 8 July 2021, Scheduled 10 August 2021

* Corresponding author: Jianxing Li (jianxingli.china@xjtu.edu.cn).

[1] School of Electric Power, North China University of Water Resources and Electric Power, Zhengzhou, China. [2] School of Information and Communications Engineering, Xi'an Jiaotong University, Xi'an, China.

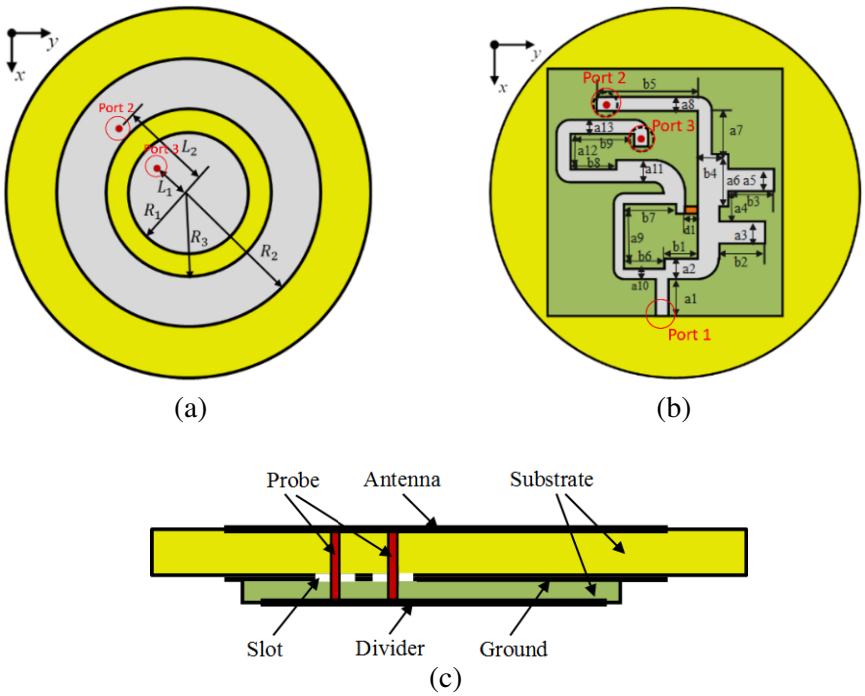

Figure 1. Configuration of proposed antenna. (a) Top antenna view. (b) Back divider view. (c) Side view.

The metal ground plane is printed on the bottom with a radius of 38 mm. The resonant frequency is mainly determined by the size of the inner circular patch, which is calculated by Eq. (1).

$$R = \frac{87.94}{f_r\sqrt{\varepsilon_r}} \tag{1}$$

After CST modeling and simulation, for center frequency (f_r = 2.54 GHz), R_1 = 13.1 mm, R_2 = 30.1 mm, R_3 = 18.7 mm, L_1 = 4.5 mm, L_2 = 19.7 mm. Two coaxial probes feed the inner patch and outer ring independently. The maximum gain direction of the inner circular patch is in the Z direction, but the pattern of the outer ring is a null point in the Z direction and omnidirectional radiation on the XY plane. The combination of the two patterns can theoretically achieve a wider HPBW, which is shown in Figure 2.

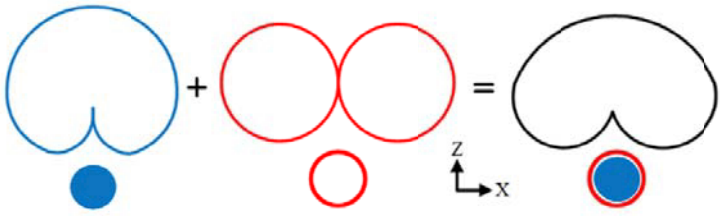

Figure 2. Wide HPBW theory of proposed antenna.

It is noted that when the outer ring has greater excitation power than the inner patch, the wide HPBW is easier to realize. Table 1 shows the HPBWs with different power ratios between inner circular patch and outer ring. We design a 1 : 5 unequal power divider to feed the inner patch and outer ring because it can broaden the HPBW better.

Figure 3 shows the simulated radiation patterns at central frequency (2.54 GHz) of only inner circular patch (a), only outer ring (b), and proposed antenna when the power ratio of the inner patch and outer ring is 1 : 5 (c). It is noted that the HPBW has been broaden obviously.

Table 1. The HPBWs of different power ratios of the inner patch and outer ring.

	Conventional circular patch	1 : 1	1 : 2	1 : 3	1 : 4	1 : 5
XZ-plane	90°	114°	121°	138°	180°	253°
YZ-plane	90°	118°	124°	145°	196°	261°

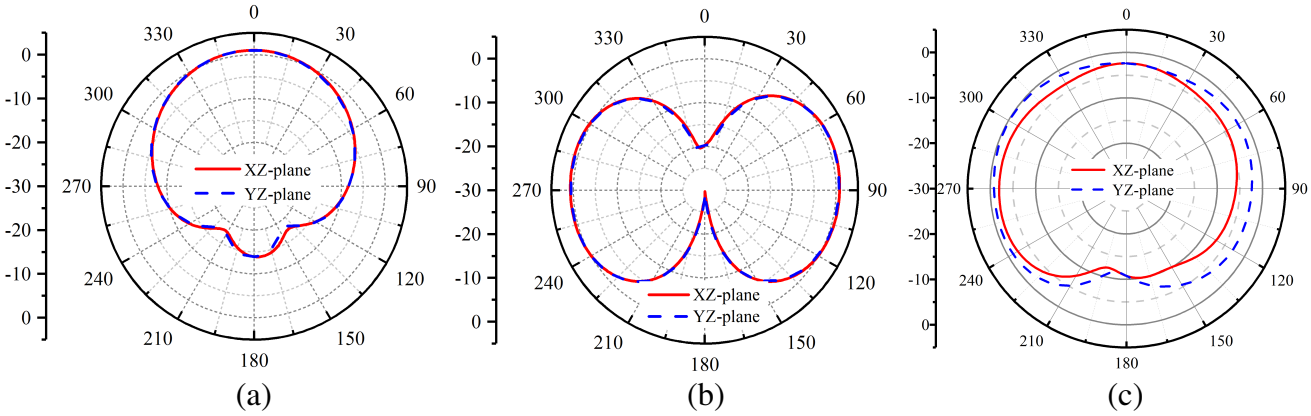

Figure 3. Simulated radiation patterns. (a) Inner circular patch. (b) Outer ring. (c) Combination.

3. POWER DIVIDER DESIGN

Due to simple structure, Wilkinson power dividers are widely used in a lot of microwave equipment. In this paper, a 1 : 5 unequal Wilkinson power divider is designed to feed the antenna.

The improvement factor C is introduced to reduce the part with large characteristic impedance, and the T-type equivalent circuit is further selected to narrow the microstrip line with small characteristic impedance. The characteristic impedance calculation after the introduction of C is as follows:

$$Z_{03} = \frac{\sqrt{Z_0(1+K^2)C}}{K} \tag{2}$$

$$Z_{02} = K\sqrt{Z_0(1+K^2)C} \tag{3}$$

$$R = (1+K^2)C \tag{4}$$

$$Z_4 = K\sqrt{Z_0C} \tag{5}$$

$$Z_5 = \sqrt{Z_0C} \tag{6}$$

Through the cascading properties of the transmission matrix, two T-shaped structures are introduced to replace the microstrip line with small characteristic impedance. Assume that the equivalent characteristic impedance of the T-shaped structure is Z_E, which satisfies

$$\begin{bmatrix} \cos\theta_A & jZ_A\sin\theta_A \\ \dfrac{j\sin\theta_A}{Z_A} & \cos\theta_A \end{bmatrix} \begin{bmatrix} 1 & 0 \\ \dfrac{j\sin\theta_B}{Z_B} & 1 \end{bmatrix} \begin{bmatrix} \cos\theta_A & jZ_A\sin\theta_A \\ \dfrac{j\sin\theta_A}{Z_A} & \cos\theta_A \end{bmatrix} = \begin{bmatrix} 1 & jZ_E \\ jY_E & 0 \end{bmatrix} \tag{7}$$

The design indicators of the power divider are as follows: central frequency $f_0 = 2.5\,\text{GHz}$, the power distribution ratio is 1 : 5, so $K = \sqrt{5}$, $Z_0 = 50\,\Omega$, and $C = 7\,\Omega$. The input selects $50\,\Omega$ equivalent impedance of microstrip line, and $C = 7\,\Omega$ is selected. The equivalent impedance of the microstrip line by type (2) to type (6) is calculated: $Z_{02} = 102.5\,\Omega$, $Z_{03} = 20.5\,\Omega$, $Z_4 = 41.8\,\Omega$, $Z_5 = 18.7\,\Omega$. The T-type equivalent structure satisfies:

$$\tan\theta_{A3} = \tan\theta_{A5} = 0.5 \tag{8}$$

$$\tan\theta_{B3} = \tan\theta_{B5} = 2\cot\theta_{A3} = 1.5 \tag{9}$$

It is calculated that

$$Z_{A3} = Z_{B3} = 2Z_{03} \tag{10}$$

$$Z_{A5} = Z_{B5} = 2Z_5 \tag{11}$$

At this point, the impedance in the equivalent circuit meets the processing level of the common process, and the characteristic impedance pairs before and after optimization are shown in Table 2. The topology of proposed divider is shown in Figure 4.

Table 2. The characteristic impedance between conventional and proposed structure.

	Conventional structure	Proposed structure
Maximum value of characteristic impedance	183.1 Ω	102.5 Ω
Minimum value of characteristic impedance	33.4 Ω	37.4 Ω
Ratio of maximum and minimum characteristic impedances	5.5 : 1	2.7 : 1

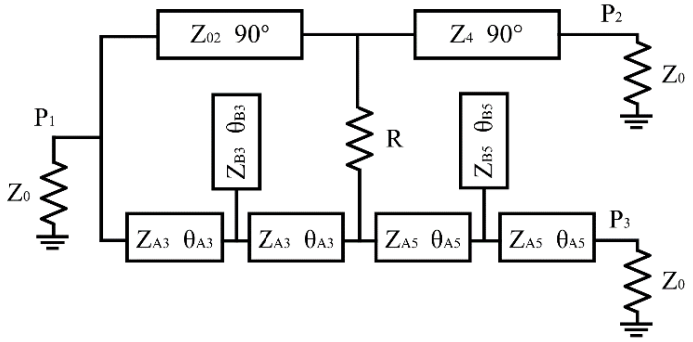

Figure 4. Topology of proposed 1 : 5 unequal Wilkinson power divider.

The substrate is Rogers RO4350 ($\varepsilon_r = 3.66$, $\tan\delta = 0.004$) with a thickness of 1.524 mm. The specific parameters of the microstrip line are calculated by the calculation tool in ADS, and the CST simulation software is used for modeling and simulation. Figure 1(b) shows the structural model of Wilkinson power divider with a 1 : 5 unequal power ratio. The isolation resistance is 43 Ω. Table 3 shows the structural parameters of proposed divider.

Table 3. Structural parameters of proposed 1 : 5 unequal Wilkinson power divider.

Parameter	$a1$	$a2$	$a3$	$a4$	$a5$	$a6$	$a7$	$a8$
Value (mm)	5	4.3	4.9	3.2	4.5	7.2	14.3	3.3
Parameter	$a9$	$a10$	$a11$	$a12$	$a13$	$b1$	$b2$	$b3$
Value (mm)	11.6	1.4	4.4	8.4	3.3	3.95	10.9	10.8
Parameter	$b5$	$b6$	$b7$	$b8$	$b9$	$d1$		
Value (mm)	20.9	5.15	5.1	6	14	2		

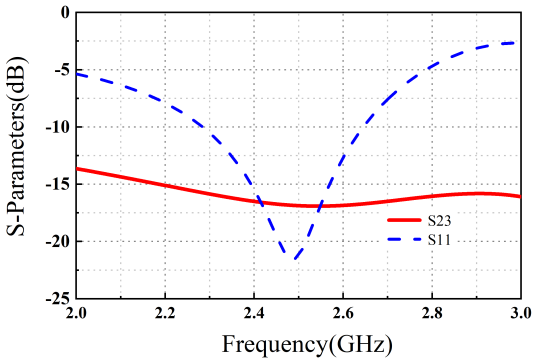

Figure 5. Reflection of port 1 and isolation of Port 2 and 3.

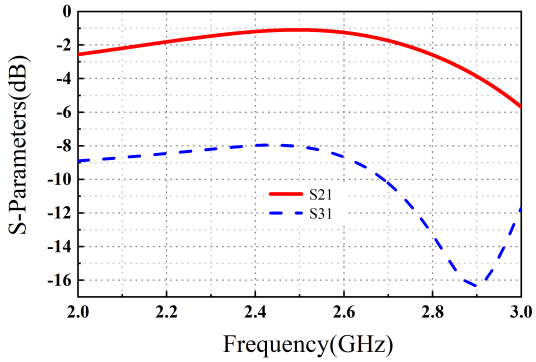

Figure 6. Insertion loss of Port 2 and 3.

Figure 5 shows the reflection coefficient curve of the power divider and the isolation between ports 2 and 3. Between 2.28 GHz and 2.65 GHz, the reflection coefficient $S_{11} < -10$ dB, and the isolation $S_{23} < -15$ dB. Figure 6 shows the insertion loss of ports 2 and 3. At the central frequency 2.54 GHz, $S_{21} < -1.09$ dB, $S_{31} < -8.05$ dB which means that power ratio between two ports is $5:1$.

4. SIMULATION AND MEASURE RESULTS

The microstrip patch antenna with low profile wide beam is shown in Figure 7. The power divider is placed on the back of the antenna, and two metal posts pass through the dielectric substrate. Compared with conventional microstrip antennas, the dielectric substrate layer extends outwards relative to the metal ground. In this way, the dielectric substrate also participates in radiation, and its maximum direction of radiation is in the horizontal plane. Combined with the radiation direction of microstrip antenna, a wider beam width is realized.

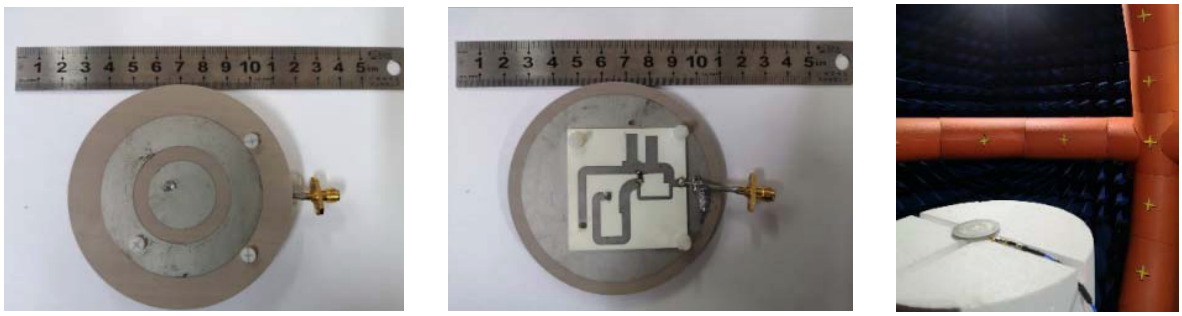

(a) (b) (c)

Figure 7. Fabricated proposed antenna and measure. (a) Top view. (b) Back view. (c) Antenna measure.

In order to verify the effectiveness of beamwidth broadening, the antenna is fabricated and tested. Figures 7(a) and (b) show the images of the antenna and the $1:5$ Wilkinson power divider. The wide beam microstrip antenna with low profile is placed back to back by the first two structures, and the two parts are connected by a welded metal post with a diameter of 1 mm. The coaxial line with SMA connector is used to feed the power divider, and the energy is transmitted from the output port of the power divider through the metal post to feed the antenna to radiate the wide beam.

CST software is used to simulate and Agilent E8363B vector network analyzer used to measure S_{11} of the proposed antenna. Figure 8 shows the reflection coefficient curves of the proposed antenna. It

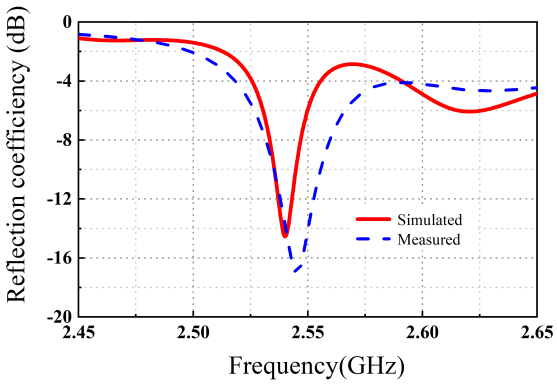

Figure 8. Reflection coefficient curves of the proposed antenna.

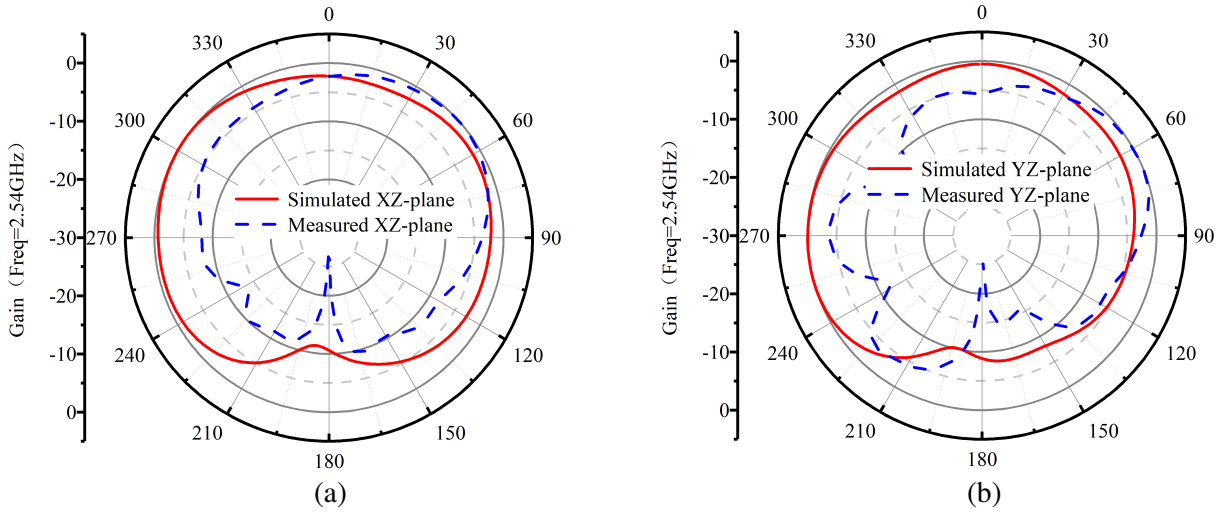

Figure 9. Normalized far field radiation gain patterns of proposed antenna. (a) XZ-plane. (b) YZ-plane.

can be seen from the figure that the simulated resonant frequency of the antenna is 2.54 GHz, and the −10 dB bandwidth is 0.55% (2.534 ∼ 2.548 GHz). The measured resonant frequency is 2.545 GHz, and the −10 dB bandwidth is 0.82% (2.535 ∼ 2.556 GHz). The trend is consistent. However, it is noticed that the measured impedance bandwidth is wider than in simulation. In the actual processing and assembly, the antenna and power divider are connected by soldering tin. The microwave energy passes through the power divider to one side of the antenna via a welded metal probe. The solder joint is not perfect, which causes energy leakage and loss. This energy will not contribute to the return loss, so the bandwidth of the actual processed antenna is wider.

A microwave anechoic chamber is used to test the proposed antenna, which is shown in Figure 7(c). Figure 9 shows the normalized far-field radiation gain pattern of the proposed antenna at the central frequency (2.54 GHz). The simulated half-power beamwidth is effectively expanded on both XZ and YZ planes, reaching 258° and 267°, respectively, covering the whole upper half space. The results show that the half-power beamwidth of the antenna can be effectively extended by loading the circular metal ring structure and extending the dielectric substrate. Figure 10 shows the realized gain of fabricated antenna within the impedance bandwidth. Due to the broadening of the half power beam width, the energy radiates to a wider angular region, and the maximum gain drops to about 0 dBi.

Table 4 shows the comparison between the proposed antenna and other previous works. It is noted that the proposed antenna has great advantages in wider HPBW and lower profile.

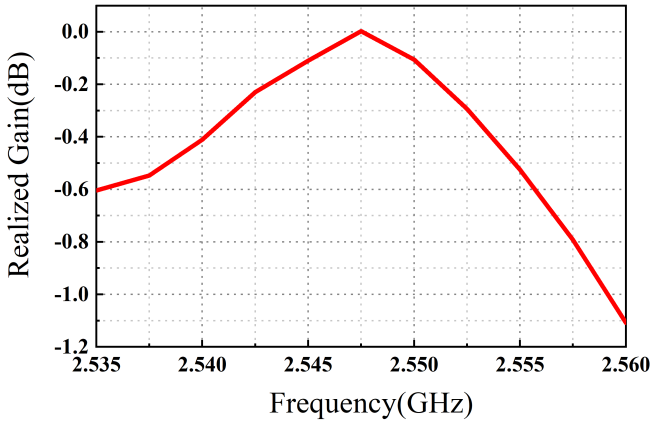

Figure 10. Realized gain within impedance bandwidth.

Table 4. Comparison of the proposed antenna with previous work.

	IMBW	HPBW	Profile
Conventional patch	3.56%	90°	
Ref. [7]	1.2%	140°	$0.11\lambda_0$
Ref. [8]	0.54%	118°	–
Ref. [9]	30%	107°	$0.16\lambda_0$
Ref. [12]	5.8%	170°	$0.073\lambda_0$
Proposed	0.55%	258°/267°	$0.027\lambda_0$

5. CONCLUSION

A low profile wide beam microstrip patch antenna fed by a 1 : 5 unequal Wilkinson power divider is designed. The half-power beamwidth of the antenna reaches 258° and 267° in XZ-plane and YZ-plane, respectively, covering the whole upper half space. The measured results show great consistency with simulated ones. In summary, the proposed antenna can be a proper antenna for some RFID systems.

REFERENCES

1. Sung, Y., "Dual-band circularly polarized pentagonal slot antenna," *IEEE Antennas and Wireless Propagation Letters*, Vol. 10, 259–261, 2011.
2. Li, J., H. Shi, H. Li, and A. Zhang, "Quad-band probe-fed stacked annular patch antenna for GNSS applications," *IEEE Antennas and Wireless Propagation Letters*, Vol. 13, 372–375, 2014.
3. Li, J., H. Huo, J. Chen, S. Zhu, H. Shi, and A. Zhang, "Miniaturised artificial magnetic conductor and its application in unidirectional circularly-polarized slot antenna design," *IET Microwaves Antennas & Propagation*, Vol. 12, No. 12, 1885–1889, 2018.
4. Yang, K. P. and K. L. Wong, "Dual-band circularly-polarized square microstrip antenna," *IEEE Trans. Antennas Propag.*, Vol. 9, 377–382, 2001.
5. Liao, W. and Q.-X. Chu, "Dual-band circularly polarized microstrip antenna with small frequency ratio," *Progress In Electromagnetics Research Letters*, Vol. 15, 145–152, 2010.

6. Yang, W. J., Y. M. Pan, and S. Y. Zheng, "A low-profile wideband circularly polarized crossed-dipole antenna with wide axial-ratio and gain beamwidths," *IEEE Trans. Antennas Propag.*, Vol. 66, 3346–3353, 2018.
7. Pan, Z. K., W. X. Lin, and Q. X. Chu, "Compact wide-beam circularly polarized patch antenna with a parasitic ring for CNSS application," *IEEE Trans. Antennas Propag.*, Vol. 62, 2847–2850, 2014.
8. Patel, R. and K. J. Han, "Utilization of higher-mode resonance in broadening the E-plane HPBW of printed antenna for automotive radar application," *2015 International Workshop on Antenna Technology (iWAT)*, 330–332, Seoul, 2015.
9. Chen, L., T. L. Zhang, C. Wang, and X. W. Shi, "Wideband circularly polarized microstrip antenna with wide beamwidth," *IEEE Antennas and Wireless Propagation Letters*, Vol. 13, 1577–1580, 2014.
10. Jorgensen, E., B. K. Nielsen, O. Breinbjerg, and M. Lumholt, "A cavity backed crossed-slot antenna element for an S-band circular polarization spherical coverage satellite antenna system," *Proc. Int. Symp. Antennas Propag.*, Vol. 1, 361–364, Fukuoka, Japan, 2001.
11. Bao, X. L. and M. J. Ammannt, "Dual-frequency dual circular-polarized patch antenna with wide beamwidth," *Electron. Lett.*, Vol. 44, 1233–1234, 2008.
12. Shi, H., J. Shi, J. Li, J. Chen, Z. Li, and S. Zhu, "Miniaturized circularly polarized patch antenna using coupled shorting strip and capacitive probe feed," *AEU-International Journal of Electronics and Communications*, Vol. 98, 235–140, 2019.
13. Sheng, X., J. Li, H. Huo, J. Chen, and A. Zhang, "Low profile unequally dual-feed circularly polarized patch antenna with a wide beamwidth," *2019 International Conference on Microwave and Millimeter Wave Technology (ICMMT)*, 1–3, Guangzhou, China, 2019.